

## **Structural Design of a Semi-Submersible Platform with Water-Entrapment Plates Based on a Time-Domain Hydrodynamic Algorithm Coupled with Finite-Elements**

*Alexia Aubault*

*Christian A. Cermelli*

*Dominique G. Roddier*

Marine Innovation & Technology  
Berkeley, California

### **ABSTRACT**

This paper discusses the structural analysis of a semi-submersible-type platform with heave plates at the base of each column, designed to develop marginal fields in ultra-deepwater. The geometry consists of three vertical rectangular columns and three pontoons with large horizontal skirts extending in all directions from the base of the columns. The skirts are subjected to significant hydrodynamic forces due to diffraction-radiation loads and viscous effects around their edges. Both extreme and fatigue analyzes of the structural members are necessary to ensure the integrity of the structure and the optimization of the hull weight. Due to the novel geometry, the modes resulting in the largest stress levels are expected to differ from conventional semi-submersible design. A systematic approach is implemented to determine the design load cases. This work highlights the necessity to run a comprehensive structural analysis combined with a hydrodynamic model in order to assess all possible failure modes.

**KEY WORDS:** Finite-elements; time-domain hydrodynamics; semi-submersible with water-entrapment plates; structural analysis.

### **INTRODUCTION**

This paper discusses the design methodology for structural sizing of a minimal floating offshore platform consisting of a three-column semi-submersible with large water-entrapment plates extending horizontally from the base of the columns. The water-entrapment plates are designed to control the platform dynamic properties, such as resonant periods in heave, pitch and roll. Therefore, even with a small payload, and small displacement, the platform exhibits the same motion characteristics as semi-submersible platforms which are 5 times larger. The platform is intended for use in the development of marginal fields in deep and ultra-deepwater.

The platform is designed in accordance with ABS Guide for Building and Classing Floating Production Installations. As such, a rigorous approach is required to perform structural engineering calculations. In addition to the water-entrapment plates, unusual features of the platform include its overall triangular shape, and the rectangular cross-

section of the stabilizing columns.

The water-entrapment plate increases considerably the platform added-mass in the vertical direction. The platform draft varies between 30 and 80 ft depending on the required topsides load. Because of the relatively shallow draft, wave excitation forces on the water-entrapment plates cannot be neglected. The relative motion between the platform and the wave kinematics results in additional viscous loads due to vortex shedding. In summary, the water-entrapment plates, also referred to as “skirts” in this paper, are subject to complex hydrodynamic loading resulting from radiation forces, diffraction forces, and viscous shedding forces.

The platform response is computed using a time-domain hydrodynamic software tool described by Cermelli et al. (2004). A semi-empirical viscous model, based on Morison equation and experimental results by Prislín et al. (1998) is implemented to compute the nonlinear viscous forces generated at the edges of the water-entrapment plates. The time-domain method allows for accurate implementation of the viscous model in random waves. A structural design approach that is consistent with the time-domain hydrodynamic model is proposed herein.

Chen and Mills (2005) reviewed the current practice and state-of-the-art methodologies for structural analysis of floating platforms. They describe the time-domain approach as more accurate and straightforward because the number of assumptions used to derive design load cases is smaller than in the more commonly-used frequency-domain approach. A limitation is noted, however, in the derivation of the radiation pressure due the formulation of memory effects. This problem is avoided here because of the assumptions used in the time-domain solution as explained in a section below.

The focus of this paper is limited to the in-place strength and fatigue analysis of the hull. The methodology can easily be adapted to transit and installation modes. Preliminary sizing of the deck structural steel is conducted as part of this work, but no load cases were specifically generated to ensure robustness of the design of primary deck tubular members.

## METHODOLOGY

Main steps of the structural design methodology and their sequence are shown in Fig. 1. A brief description of each step is given below:

**1. Global sizing: payload, stability.** The main platform dimensions are established using a design spreadsheet. Equipment weight and riser loads are specified as input. Convergence is achieved when certain targets are reached for displacement, stability (GM) and dynamic properties (natural periods). Required data, such as mooring tension, hydrodynamic added-mass, structural deck and hull weight are based on simplified models, and extrapolations from previous runs. If the platform response, obtained from more accurate time-domain simulations (step 3) are insufficient, the spreadsheet is updated, and another series of optimizations is performed.

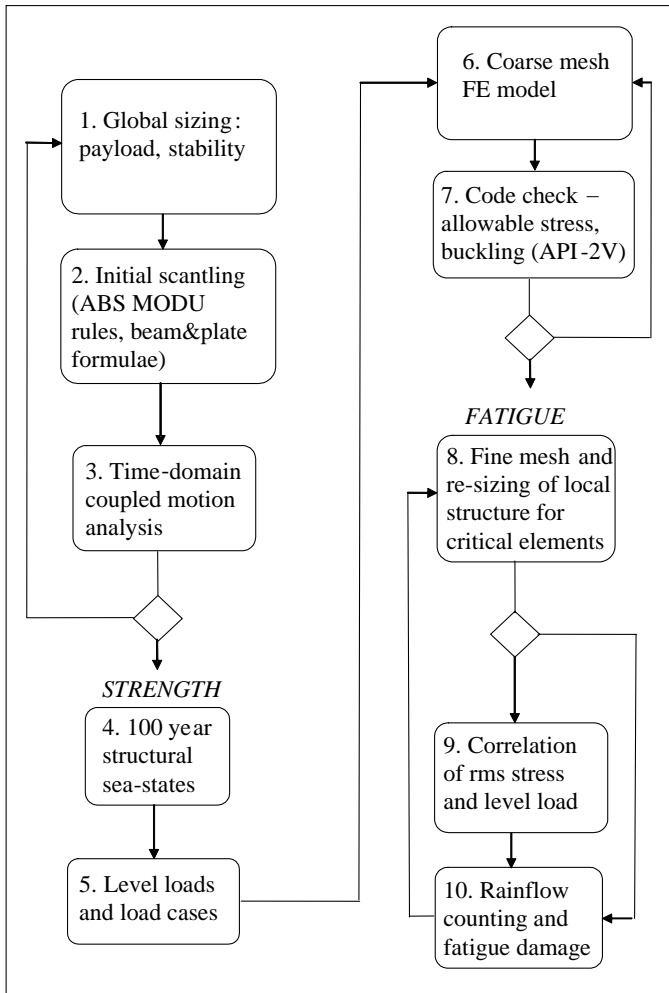


Fig. 1: Flow chart of structural design methodology

**2. Initial scantling (ABS MODU rules, beam&plate formulae).** Preliminary sizing of the columns and pontoons is carried out based on ABS MODU rules. Scantlings of the water-entrapment plates are based on simplified beam and plate stress models. Initial estimate of deck steel is also based on a simplified beam model. If substantial differences in the distribution of structural weight are observed, the global sizing step is repeated.

**3. Time-domain coupled motion analysis.** Motion analysis of the

platform coupled with the mooring lines and Steel Catenary Risers (SCR's) is performed in the time-domain. The platform responses in extreme events and maximum operating sea-states are computed and compared with acceptability criteria. The mooring system is designed in accordance with API-RP2SK and ABS Guidance Note on the Use of Synthetic for Offshore Applications. The first three steps are repeated until a satisfactory design is obtained.

**4. 100 year structural sea-states.** The largest sea-states (in term of wave height) may not generate the largest structural responses: the wave period may be the dominant parameter for some structural modes. In this step, design sea-states with periods covering the entire wave range are generated. The platform is assumed to be located in ultra-deepwater in the Gulf of Mexico. A series of Jonswap spectra was generated with peak periods ( $T_p$ ) varying between 6 and 15 seconds, and an associated significant wave height ( $H_s$ ) such that each sea-state return period is 100 year. The process followed is described in more details in a later section. It is assumed that the maximum structural response generated by these sea-states will have a 100 year return period.

**5. Level loads and load case.** Ideally, structural analysis of the platform would be conducted for all design sea-states. This is far from practical, however, because the sea-states are three-hours long, and the combination of wave heading and peak periods amount to well over one hundred sea-states, which represent a very large number of wave events. Instead, forces and moments are calculated for each time-step of these sea-states at a number of locations (levels) across the platform, such as the pontoons and column ends and mid-section and the water-entrapment plate edges and center. Various modes of structural deformation are then considered (prying mode, squeezing mode, deck acceleration mode, etc) and "snapshots" of the maximum event based on time-series of level loads are determined for each structural mode. Hydrodynamic pressures, platform motion, mooring and riser loads are stored for each snapshot.

**6. Coarse mesh FE model.** A coarse mesh quasi-static finite-element model is generated for the various snapshots. Pressure loads and external forces (mooring, risers) are applied to the model.

**7. Code check - allowable stress, buckling (API-2V).** Von Mises stress is compared to allowable values, and structural stability checks are conducted on the hull plating and stiffeners using API-2V formulation. The structural model is modified until all criteria are satisfied. If structural weights are too far from the results of the initial global sizing phase, then the process may be repeated. Conservative estimates of steel weight in the initial sizing phase are recommended to reduce the amount of re-design.

**8. Fine mesh and re-sizing of local structure for critical elements.** Analysis of the hot-spot stress is then carried out by generating a fine mesh model at critical locations. Guidance on the required mesh size can be found in ABS Guide for the Fatigue Assessment of Offshore Structures (2003).

**9. Correlation of rms stress and level load.** Because it is not possible to conduct systematic structural analysis for all fatigue sea-states, a limited number of runs are conducted to establish the correlation between hot-spot stresses and level loads. The stress time-series can then be generated at these critical locations based on transfer functions of stresses applied to the time-series of level loads

**10. Rainflow counting and fatigue damage.** Rainflow counting is then performed, and fatigue damage can be determined from S-N

curves, and probabilities of occurrence of each sea-states in the wave-scatter diagram. If the fatigue life target is not reached, local re-sizing is performed.

Further details on the main steps of this design process are provided below.

### GLOBAL SIZING AND COUPLED ANALYSIS

A time-domain numerical algorithm was developed to compute the response of the platform. The formulation and validations are presented in Cermelli et al., 2004. The algorithm main steps are summarized here: the 6-Degrees-Of-Freedom equations of motion are advanced at each time step using a fourth order Runge-Kunta method. External forces are updated at each fractional time-step as follows:

- wind forces are computed based on drag coefficients and projected areas of the structure consistent with API-RP2A;
- current forces on the columns and vortex-shedding forces at the edges of the water-entrapment plate are based on a Morison equation approach taking into account the relative velocity between the platform and the water particles. Drag coefficients on the water-entrapment plate were derived from Prislin et al. and were confirmed by model test results. The model is adapted on the water-entrapment plate to only generate loads that are perpendicular to the plate.
- drift forces are computed using the Newman’s approximation applied to the mean drift coefficients computed by diffraction-radiation software WAMIT;
- mooring and risers are modeled using a finite-difference algorithm. The mooring and riser top tensions are updated at each fractional-time step, and their configuration is re-computed based on the latest vessel motions; hence vessel motion and tether dynamics are fully coupled.
- Wave-exciting force coefficients composed of the Froude-Krilov and diffraction components are calculated by WAMIT. Random-wave realizations of a Jonswap wave spectrum are created using Fourier series with randomized phases and frequency intervals.

Added-mass and wave damping coefficients, as well as hydrostatic stiffness coefficients, also computed by WAMIT, compose the left hand side of the equation of motion. The classical time-domain solution of a body in waves involves the computation of a convolution integral with a kernel composed of the so-called “retardation” functions that represent the “wave memory effects”. This step is complex as convergence of the convolution is problematic in long waves, and it is computationally demanding. An alternate method is possible here because of the assumption of “narrow-banded process”. This assumes that the variation of added-mass and wave damping coefficients is negligible within the range of frequencies of the platform response. Horizontal motions (surge, sway and yaw) are dominated by slow-drift frequencies, and the corresponding added-mass and wave damping are used. This typically results in a slight under-prediction of the overall wave damping, and is slightly conservative. Vertical motions (heave, pitch and roll) are dominated by wave frequencies, hence the added-mass and damping coefficients corresponding to the peak period of the waves are selected. Since the spectral response is typically narrow-banded, this approximation is accurate. Furthermore, damping is by far dominated by viscous effects on the water-entrapment plates, therefore wave radiation damping is only a small contribution.

The numerical algorithm was validated by model tests conducted at the University of California at Berkeley Ship Model Testing Facility. A rendering of the platform is provided in Fig. 2. The Response Amplitude Operators are plotted in Fig. 3. The agreement between

predicted motion and measurements indicate that the assumptions used in the numerical model are appropriate for all practical design purposes.

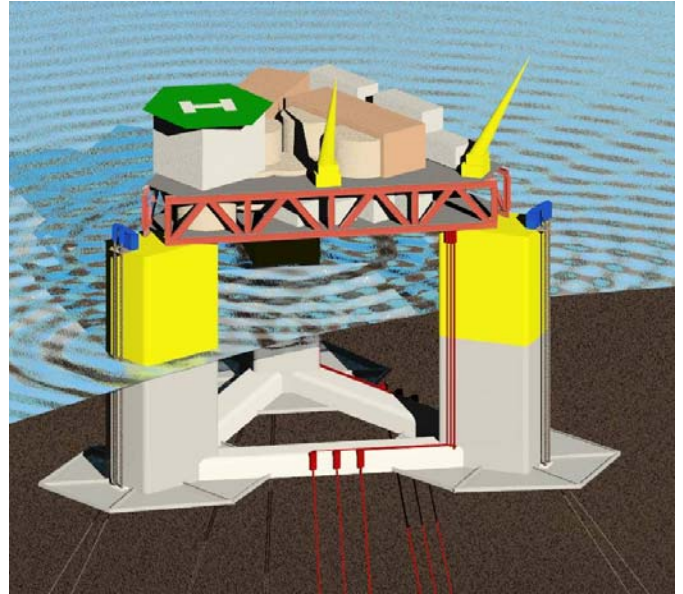


Fig. 2: Rendering of the MINIFLOAT platform with topsides equipment, mooring lines and Steel Catenary Risers

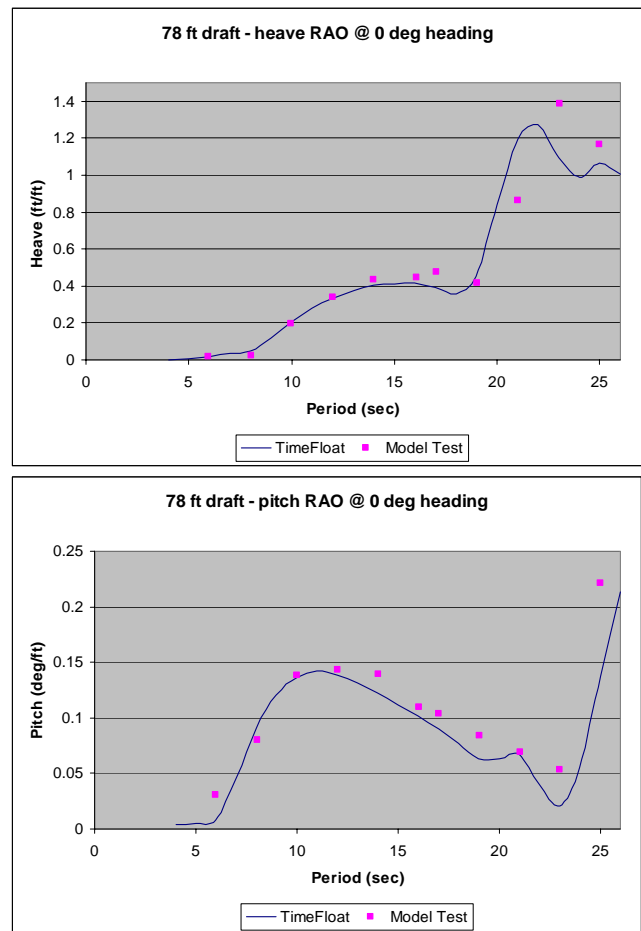


Fig. 3: Heave RAO (top) and pitch RAO (bottom). Validation of the numerical algorithm by model tests

## DERIVATION OF 100 YEAR STRUCTURAL RESPONSES

The process used to derive 100 year level structural responses is described in this section. It is based on the design wave analysis described for instance in ABS Commentary on the Rules for Building and Classing Mobile Offshore Drilling Units (2005) with adaptations consistent with the time-domain algorithm presented in the previous section.

The load cases to be considered for structural design of the platform differ somewhat from those of two-pontoons semi-submersibles as described in the MODU rules referred above. The list of load cases found to drive the structural design of the platform hull is given in Table 1:

Table 1: Load cases for structural design of the hull

Load case	Description
Pry mode	Two columns are “pulled apart” by action of a wave resulting in maximum tension load into the pontoons.
Squeeze mode	Similar to the pry mode, with wave load tending to move two columns toward each other; also maximum compressive load in the pontoons.
Maximum deck acceleration mode	Results in maximum deck inertia loads applied at the top of columns. Maximum shear of the deck supports and top of column. This mode is similar to the maximum pitch mode, but it results in higher shear at the top of column.
Maximum pontoon shear	Maximizes the differences in vertical loads at each end of a pontoon. These are mainly due to load applied to the water-entrapment plates.
Maximum skirt load	Maximum load on a water-entrapment plate tending to shear the water-entrapment plate off the base of the column.
Maximum skirt bending	Maximum bending moment on a section of water-entrapment plate between radial stiffeners

Loading on various hull members depends on wave height but it is also strongly affected by wave period. A series of “100 year sea-states” with peak periods covering the entire wave range are defined. Observations from two National Oceanic & Atmospheric Administration deepwater buoys located in central and western Gulf of Mexico (42001, 42002) covering 50 years of hourly wave data were used to derive a long-term wave scatter diagram. For each peak period between 6 and 10 seconds, a histogram of occurrences of various significant wave heights is generated; see a sample for 8 second peak period in Fig. 4. A Weibull fit of the 10% highest sea-states is then performed, and a projection to the 100 year return period level is obtained.

It is noted that there may be some correlation between the two observation sites, although they are located a few hundred miles apart, especially concerning the occurrence of winter storms. This would tend to make the analysis slightly un-conservative. On the other hand, the Weibull extrapolation performed here ignores all limiting factors, such as wave breaking or shift of energy toward longer periods. This latter simplification is therefore conservative.

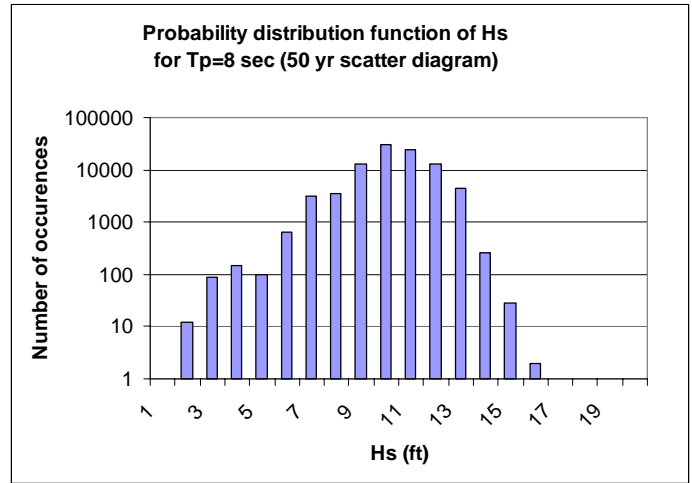


Fig. 4: histogram of significant wave heights for  $T_p=8$ sec based on a 50 year wave-scatter diagram

Periods less than 6 seconds are neglected because the corresponding waves are too small to drive the platform structural design. For periods greater than 11 seconds, there is not a sufficient number of occurrences in the 50 year wave scatter diagram to perform extrapolation. Instead, we used design values for Gulf of Mexico hurricanes (available from a variety of sources with slight variations in peak period and significant wave heights). The following values, corresponding to the high range of available data are used:  $H_s=45$  ft with  $T_p=14$  sec or  $H_s=48$  ft with  $T_p=15$  sec. The 100 year significant wave height for peak periods between 11 and 13 seconds was obtained by interpolation. The resulting set of 100 year sea-states are given in Table 2.

Associated wind and current conditions were selected as follows: ten year return period winter storm wind and associated current values were used for periods up to 11 seconds. It was assumed that all sea-states below 11 seconds were transient conditions resulting from a 10 year winter storm wind. Larger sea-states come from hurricanes, and associated wind and current speed were interpolated from 100 year associated design conditions.

Table 2: 100 year sea-states for varying peak periods

Peak period ( $T_p$ )	Sig. wave height ( $H_s$ )	Wind speed ( $V_w$ )	Current speed ( $V_c$ )
6 sec.	12 ft	37 kn	0.7 kn
7 sec.	15 ft	37 kn	0.7 kn
8 sec.	17 ft	37 kn	0.7 kn
9 sec.	21 ft	37 kn	0.7 kn
10 sec.	25 ft	37 kn	0.7 kn
11 sec.	30 ft	46 kn	1.3 kn
12 sec.	35 ft	54 kn	1.9 kn
13 sec.	40 ft	63 kn	2.4 kn
14 sec.	45 ft	71 kn	3.0 kn
15 sec.	48 ft	80 kn	3.6 kn

For simplicity, the Steel Catenary Risers were ignored, which led to a 120 degree symmetry of all results (the topsides loads were also assumed to be symmetric). As a result, only three wave heading were run:

- 0 deg (wave coming in between columns)
- 90 deg (wave direction aligned with two columns)
- 180 deg (wave coming in one column)

0 and 180 deg cases are also port and starboard symmetric.

Time-domain simulations of the platform response in design sea-states were conducted assuming one-hour event duration. This is somewhat un-conservative for hurricane conditions, which are typically considered stationary over a 3-hour interval. This would be rectified in a detail design phase, however it is believed to yield sufficient accuracy in the present conceptual stage.

Simultaneously with the motion solver, the pressure field is calculated at each hydrodynamic panel on the structure. Diffraction pressure is integrated over the wetted-hull to verify that the global wave force obtained is identical to the wave-exciting force component provided by WAMIT. The radiation pressure is simply obtained by multiplication of the body motion (acceleration for the added-mass part, velocity for the radiation damping part) by the frequency-domain pressure coefficients at the selected period (see section on the time-domain numerical algorithm). Again, it can be verified that the hydrodynamic inertia component is identical to the integral of the radiation pressure, and similarly for the wave damping component. It is noted that diffraction-radiation simulations are conducted using a source formulation, and a finite thickness (0.5 ft) for the water entrapment plate.

Viscous forces generated at the edges of the water-entrapment plate are converted into hydrodynamic pressure by assuming that they are spread over the row of hydrodynamic panels adjacent to the edge of the plate. A sample hydrodynamic pressure output is shown in Fig. 5. Areas of low pressure on the outside of the columns and high pressure on the inside generate the maximum load in this mode.

Pressures are integrated at sections across the main structural elements (pontoons and column ends and mid-section), and on each of the six sectors of the hexagonal shaped water-entrapment plates. Resulting “level loads” affecting the structural load cases of Table 1 are then computed in the time-domain for each of the 100 year structural design sea-states. Sea-states driving each of the modes are given in Table 3.

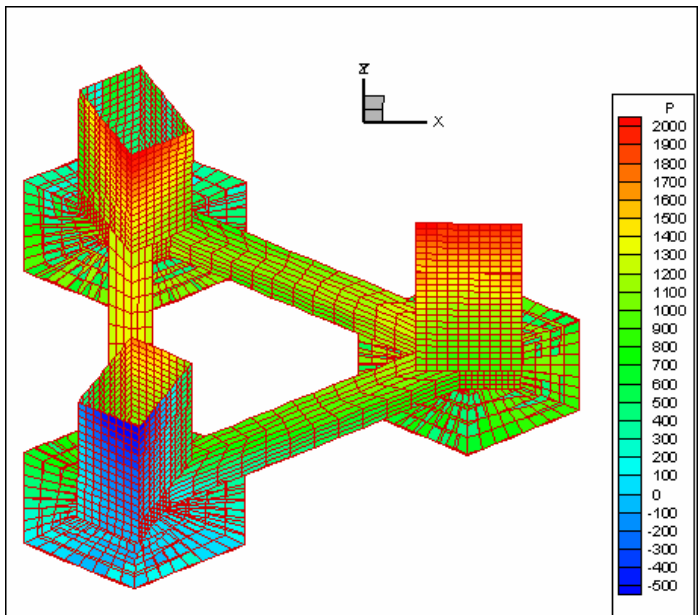


Fig. 5: hydrodynamic pressure field in the pry mode – pressure is shown in lbs/ft<sup>2</sup>

As an example, the maximum pry load recorded for each design sea-state is plotted in Fig. 6 as a function of peak period. This confirms that wave periods smaller than 6 seconds are irrelevant for this mode,

and also that there is less than 10% difference in pry load for sea-states between 11 and 15 seconds.

Expectedly, pry modes and squeeze modes are maximum in 90 deg wave heading, since it corresponds to the case where the waves travel in the same direction as the pontoon axis. It is also noted that the largest sea-state generates the largest load on the water-entrapment plate.

Table 3: design sea-states for each load case

Load case	Tp (sec)	Hs (ft)	Wave heading (deg)
Pry mode	40	13	90
Squeeze mode	35	12	90
Maximum deck acceleration mode	45	14	0
Maximum pontoon shear	40	13	180
Maximum skirt load	48	15	0
Maximum skirt bending	48	15	0

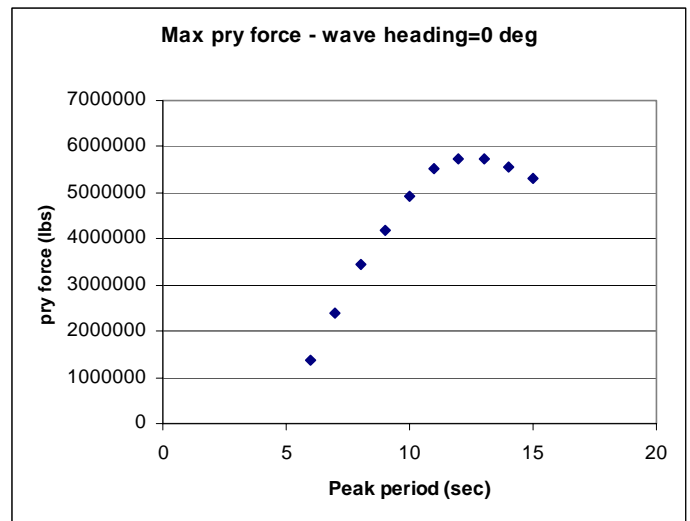


Fig. 6: pry load as a function of the design sea-state

### STRENGTH ANALYSIS

Pressure fields corresponding to the sea-states in Table 3 are saved for the time-step that generates the worst response. Mooring tensions and body motion are also stored to be entered in the quasi-static finite-element model.

Although pressures and platform motions are determined in the time-domain, it is not necessary to run a dynamic finite-element model, since the exciting forces in the numerical model contain only minimal amounts of energy for periods smaller than the lowest wave period (set to 3.5 seconds in the model) that may cause structural resonance of some panels. This is not to say that actual viscous forces on the edges of the plate do not contain high frequency spikes as vortices are shed, however this is not considered in the Morison-type model used in the present algorithm. A specific study will have to be conducted to show that panels in the vicinity of the plate edges have a resonant frequency that is much higher than that of the vortex shedding spikes.

A finite-element model of the platform is generated, with 6-nodes triangular plate elements to model the hull outer shell, and the various girders, flats and bulkheads and beam elements to model stiffeners and deck structural beams. A variety of finite-element programs may be used to conduct this type of analysis. This work was carried out with Code\_Aster software version 7 (2005) developed by Electricité De France (EDF) and used for a variety of structural and civil engineering applications, such as design of dams, nuclear power plants, transmission lines, rotating equipment, offshore wind turbines, etc.

The mesh generated for the strength analysis is shown in Fig. 7 for the maximum deck acceleration mode. The displacements have been amplified by a factor of 100. The mesh is composed of 60,000 elements.

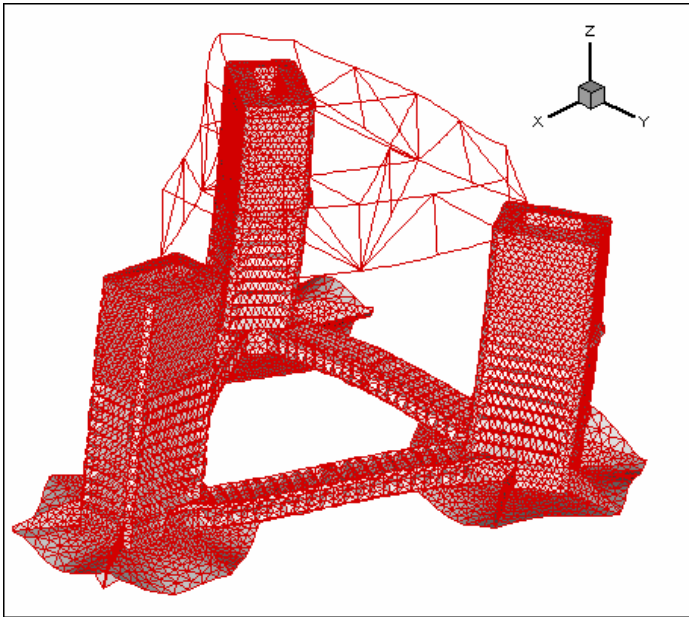


Fig 7: Deformed mesh for maximum deck acceleration mode – displacements amplified 100 times

Von Mises stresses are checked throughout the entire structure. Sample plots are provided in Figs 8, 9 and 10 for the maximum skirt load case. Areas of relatively high stress include the deck/top of column connection, the pontoon/column connection (Fig 8). The columns are internally reinforced with horizontal frames every six feet (Fig 9). The columns are 48 x 32 ft on the outside, with a 28 x 12 ft inner shaft, allowing access to the lower parts of the hull. Frames are made of girders with 4 x 6 ft openings. The highest stresses in the platform are localized around the edges of the openings with values exceeding the allowable in the lower 2 frames. Local stiffening will be required in these areas.

The water-entrapment plate is hexagonal in shape (Fig 10). Two corners are supported by the pontoons, and the remaining four corners by radial stiffeners extending from the column. The stiffeners are 12 ft high at the columns (same height as the pontoons) and they are tapering off at the edges of the water-entrapment plate. They are also modeled using plate elements. The water-entrapment plate and the radial stiffeners are stiffened panels with two sets of orthogonal stiffening members. These members are not modeled but their inertia is accounted for in the finite-element model. Stress levels in the water-entrapment plate are very low, however the maximum displacement is 40 mm (1.57”) which corresponds to a 1/500 ratio over the length of

the water-entrapment plate edge.

With the exception of localized hot-spots around the edges of the lower two frames inside the columns as noted above, the highest Von Mises stress is 150 MPa (21.7 ksi) at the connection of the radial stiffener with the column. This yields a safety factor of 1.66 with 36 ksi steel, which is allowable using a 1/3 increase in allowable for this 100 year event.

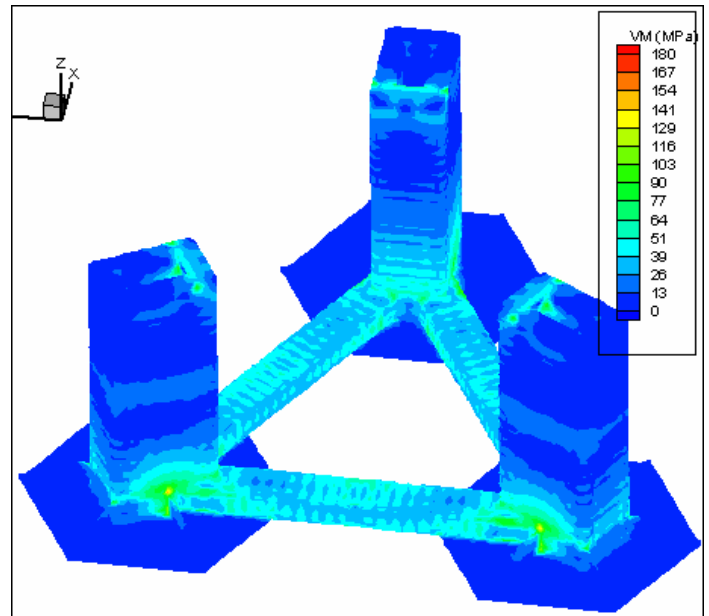


Fig 8: Von Mises stress in maximum skirt load case

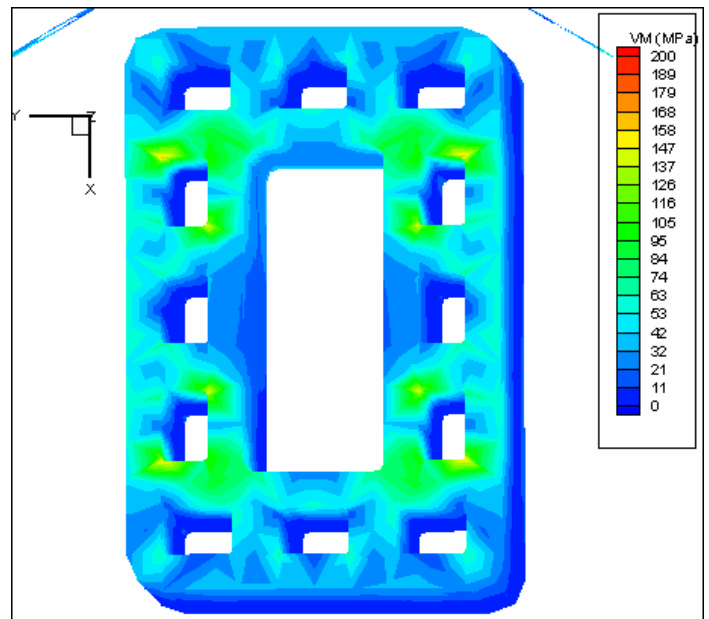


Fig 9: Stress in column 1 frames – maximum skirt load case

Buckling verifications are conducted using guidelines set by API Bulletin 2V for the design of flat plate structures. Maximum stress, deflection and load, including hydrodynamic pressure at various locations are post-processed to verify the serviceability limit state of the following critical elements:

- column/pontoon outer shell simply supported by girders every 6 feet with longitudinal stiffeners every 2 feet

- 4 foot wide girders between openings in column frames

Stiffening members of the water-entrapment plate are designed in accordance with the section on stiffened panel. The radial beams supporting the edges of the water-entrapment plates are stiffened in accordance with the section on deep plate girders. Openings will be made on the radial stiffener to limit pressure differences between the two sides of the stiffener. Due to the complex geometry, finite-element modeling of all the stiffeners and openings on the side of the radial stiffeners is recommended for detail design.

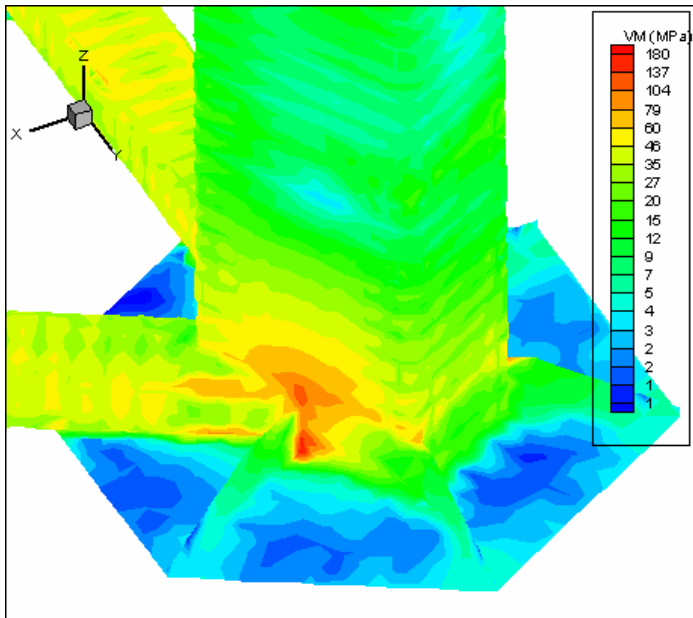


Fig 10: Stress in water-entrapment plate – maximum skirt load case

## FATIGUE ANALYSIS

Among the high stress areas, the most fatigue-prone location (hot-spot) is the connection of the radial stiffeners supporting the water-entrapment plate to the column. Details of the methodology to be used for fatigue analysis can be found in ABS Guide for the Fatigue Assessment of Offshore Structures (2003).

A fine mesh finite-element model for hot-spot stress is generated. Although triangular-shaped elements are not recommended for this type of modeling, there was no other option available with the mesher provided in the finite-element package used for this work. Fig. 11 shows the mesh at the connection of the radial stiffener with column side. The size of the finest elements is similar to the thickness of plating at the connection. Only one stiffener was modeled with a fine mesh.

The 50 years wave-scatter diagram described above consists of 12 period bins, with peak period between 1 and 12 seconds, and 24 Hs bins, with Hs between 1 and 24 ft; however, only 97 combinations of Hs and Tp have a non-zero probability of occurrence. The wave-directionality information was not processed in this analysis, so it was assumed that all headings were impacted with the same distribution of sea-states. One-hour time-domain simulations were run for three headings (0, 90 and 180 deg wave heading) for each one of the sea-states in the wave-scatter diagram. This process is time-consuming (several days worth of CPU on a modern PC), but it does not require

solution of the FE model. The integrated level loads are processed at the same time, so that there is no need to save the pressure field at each time-step.

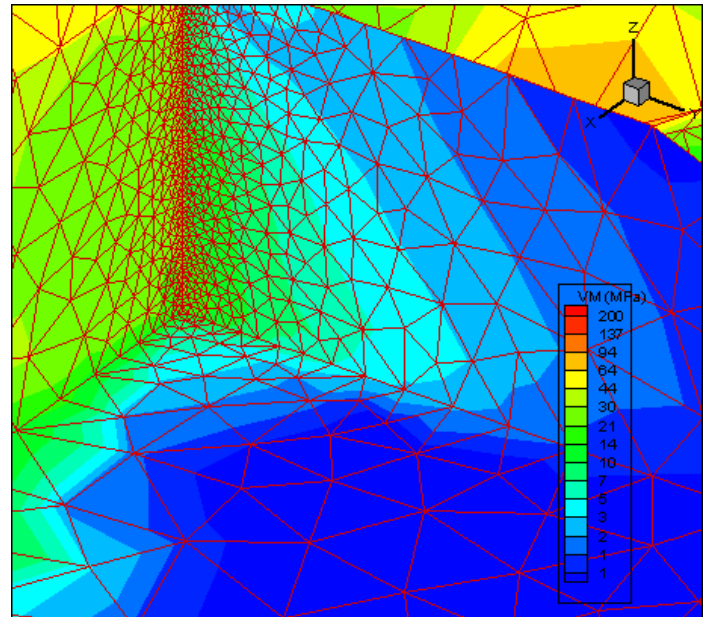


Fig 11: Fine mesh detail of the radial stiffener at the connection with column

Finite-element solutions were obtained from a dozen of snapshots representing a variety of loading conditions on the radial stiffener. The pressure fields were output only for these snapshots. The maximum stress, which occurs at the corner of the stiffener/column side/water-entrapment plate, was re-interpolated from stresses at the first and second nodes away from the corner. A sample result of stress at the hot-spot is provided in Fig. 11 for one of the fatigue load cases.

Correlation was then calculated between the maximum stress and the level load on the radial stiffener. In this case, the level load corresponds to the half sum of bending moment on each water-entrapment panel adjacent to the radial stiffener (obtained by integration of the dynamic pressure fields on each panel). Excellent correlation was found at this specific location between the maximum stress and the level load. The correlation coefficient is equal to 0.97.

Since time-series of the level load were available for each sea-state, and because of the high correlation with maximum stress at the connection, stress time-series could be generated for all sea-states without performing a large number of finite-element calculations.

A Rainflow algorithm was used to establish the long-term distribution of stress cycles. Since the wave scatter diagram represents 50 years of data, this corresponds to 150 years of life exposure for the three headings. The number of cycles was therefore corrected for the 20 year life target. The following SN curve based on ABS Guide for the Fatigue Assessment of Offshore Structures (2003) was selected for evaluation of the connection fatigue performance: ABS-(CP) Detail Class 'F' (Fig. 12). The Palmgren-Miner's rule is then used to estimate damage from each stress range bin. The resulting cumulative damage is computed by summing all bins.

Design life of the connection is estimated at 1450 years, which corresponds to a factor of safety 72. A factor of safety of 10 is required on fatigue life because it is a critical submerged location and cannot be

repaired without decommissioning the platform. Other critical fatigue areas include the connection of the mooring lines and risers, however these are connected to strong parts of the structure (the base of the column and pontoons) and therefore they will only affect the structure locally, hence will only have a minor effect on overall structure weight.

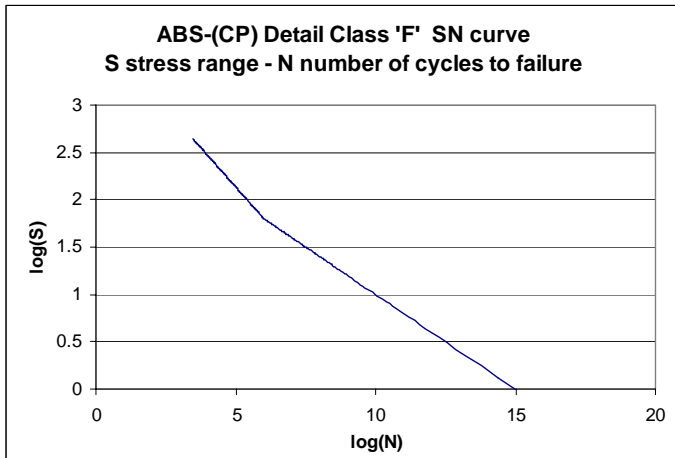


Fig 12: two-segments S-N curve used for radial stiffener/column connection

## CONCLUSIONS

A robust approach is presented to perform structural analysis of a novel floater type consisting of a small-size semi-submersible platform with large water-entrapment plates extending from the base of the columns.

Structural modeling is based on a combination of time-domain simulations of the platform hydrodynamics and finite-element analysis. Viscous effects generated by the water-entrapment plate are modeled using a semi-empirical Morison equation formulation and viscous forces are converted to a pressure distribution near the edges of the water-entrapment plate. A frequency-domain diffraction-radiation software provides the inviscid pressure on the structure.

Analysis of available wave data in the Gulf of Mexico yields a series of design “100-year” sea-states with varying peak period. Time-series of hydrodynamic loading on the structure are generated for various failure modes, and maximum events are selected for finite-element modeling.

The effects of wind, current, mooring lines and risers can be modeled without assumptions. However, for simplicity in this paper, these effects were not explicitly included in the finite-element model. Actual forces were however available from the time-domain simulations and would be included in a detail design phase.

If a strong correlation can be established between stress levels and pressure distributions in parts of the structure, fatigue analysis can be carried out consistently with very few assumptions, and with an easily manageable computer burden.

The main advantage of the present method is the ability to model with few assumptions and a relatively limited computational load, a floating structure subject to strong viscous effects coupled with wave-induced forces.

This work confirmed the structural robustness of the present design, particularly that of the large water-entrapment plate extending from the base of each column. The total hull weight determined by the analysis is 3,250 tons, which is 24% lower than the estimate used to perform the platform global design.

## ACKNOWLEDGMENTS

The authors wish to acknowledge the Code-Aster team for making their state-of-the-art finite-element software available, and the contributors to the Forum Code\_Aster for their invaluable guidance.

## REFERENCES

- American Bureau of Shipping (2003). “Guide for the Fatigue Assessment of Offshore Structures”
- American Bureau of Shipping (2004). “Guide for Building and Classing Floating Production Installations”
- American Bureau of Shipping (2005), “Rules for Building and Classing Mobile Offshore Drilling Units 2006”
- American Bureau of Shipping (2005), “ABS Commentary on the Rules for Building and Classing Mobile Offshore Drilling Units 2001”
- American Petroleum Institute (2000), “Design of Flat Plate structures” *API Bulletin 2V*
- American Petroleum Institute (2000), “Recommended Practice for Planning, Designing, and Constructing Fixed Offshore Platforms – Working Stress Design” *API RP 2A-WSD, 21<sup>st</sup> edition*
- Cermelli, CA, Roddier DG, and Busso, CC (2004). “MINIFLOAT: A Novel Concept of Minimal Floating Platform for Marginal Fields Development,” *Proc. of 14th Intl. Offshore and Polar Engrg Conf (ISOPE)*, Toulon, France.
- Chen, CY, and Mills, T (2005). “A Review of In-Place Design Approaches for Spar Hulls,” *Proc. 24<sup>th</sup> Int Conf Offsh.Mech. & Arctic Engrg.(OMAE)*, Halkidiki, Greece.
- Code\_Aster version 7 (2005) “Analysis of Structures and Thermomechanics for Survey and Research” [http://www.code-aster.org/produit\\_doc/plaq\\_V7\\_GB.pdf](http://www.code-aster.org/produit_doc/plaq_V7_GB.pdf)
- Prislin I, Blevins, RD, and Halkyard, JE (1998). “Viscous damping and added-mass of solid square plates,” *Proc. 17<sup>th</sup> Int Conf Offsh.Mech. & Arctic Engrg.*, Lisbon, Portugal